Effect of Al-dopant on Structural and Optical properties of CdS Thin Films Prepared Spray Pyrolysis Method

Y. P. Sarnikar[a], V. S. Chandak[a], A. D. Kanwate[b], L. H. Kathwate[a] *

[a]Thin Film and Materials Science Research Laboratory, Department of Physics, Dayanand Science College, Latur-413512, Maharashtra, India.

[b]Shri Vyankatesh Art's, Commerce and Science College, Deulgaon Raja, Maharashtra, India.

* *Corresponding author's E-mail address:* shkathwate1991@gmail.com

Abstract

Al-doped CdS thin films were deposited on glass substrates by spray pyrolysis with Al concentrations 0 and 1 at. %. X-ray diffraction confirmed the formation of cubic CdS with a dominant (111) preferred orientation and nanocrystalline grain size (55 nm at 1 at. % Al). Scanning electron microscopy revealed dense and uniform surface morphology, while energy-dispersive X-ray spectroscopy verified successful Al incorporation without secondary phase formation. The band gap values were found to be increased with doping. The structural stability and compositional uniformity of the films demonstrate their suitability as window/buffer layers for thin-film photovoltaic devices.

Keywords: Al-doped CdS; Spray pyrolysis; Thin films; XRD; SEM; EDS; Photovoltaic materials.

1. Introduction

Cadmium sulphide (CdS) is an II–VI group semiconductor material that has received a lot of attention because its direct band gap energy is about 2.42 eV at room temperature [1]. This makes it perfect for use in optoelectronic devices like solar cells, photodetectors, light-emitting devices, and thin-film transistors. CdS is a common window and buffer layer in heterojunction solar cells because it has a high optical absorption coefficient in the visible range. The structural quality of CdS thin films is very important for their optical and electrical performance. This is because crystallinity, lattice defects, and grain size all have a big effect on how charges move and recombine [2].

To make CdS thin films, different deposition methods have been used, including chemical bath deposition, thermal evaporation, spray pyrolysis, and sputtering[3], [4], [5]. Among these, low-cost solution-based methods stand out because they are easy to use, can be used on large areas, and are easy to scale up. But pure CdS thin films often have problems like low crystallinity,

high defect density, and uncontrolled grain growth, which can make their devices work worse. Doping with the right metal ions has been looked into a lot as a way to change the structural and electronic properties of CdS in order to solve these problems [6], [7].

Aluminium (Al) is a good dopant for CdS because its ionic radius is smaller and its valence state is higher than that of Cd^{2+} ions. Replacing Cd^{2+} with Al^{3+} can cause lattice strain, change the way crystallites grow, and affect the formation of defects. This changes the structural and functional properties of CdS thin films. Adding aluminium to a material has been shown to make it more crystalline, smaller grains, and better at conducting electricity by raising the concentration of carriers. Also, controlled Al incorporation can stop the formation of secondary phases while keeping the host CdS crystal structure intact [8], [9].

In this context, the current study concentrates on the synthesis of pure and 1% Al-doped CdS thin films, along with a systematic examination of their structural properties through X-ray diffraction (XRD). We look closely at how adding Al affects the lattice parameters, crystallite size, interplanar spacing, and phase purity. To make CdS thin films work better for advanced optoelectronic and photovoltaic uses, you need to know about these structural changes.

2. Synthesis and Characterization

2.1 Synthesis of Pure and Al-Doped CdS Thin Films

Using the spray pyrolysis method, pure and 1% Al-doped cadmium sulphide (CdS) thin films were deposited on glass substrates that had been thoroughly cleaned. Before being deposited, the glass substrates were cleaned in acetone, ethanol, and deionised water for 15 minutes each using ultrasound to get rid of dust and organic contaminants. They were then dried in the air.

For the synthesis of CdS thin film, the precursor solution was made by using cadmium acetate dihydrate as the source of cadmium and thiourea as the source of sulphur. Both precursors were dissolved separately in deionised water and then mixed together in a stoichiometric molar ratio to make a clear, even solution. To make sure that the film grew evenly, the total molarity of the solution was kept at an optimal level. To make 1% Al-doped CdS thin films, we added the right amount of aluminium nitrate nonahydrate to the precursor solution, which was equal to 1 at.% of Al compared to Cd. The solution was stirred with a magnet for an hour at room temperature to make sure it was completely dissolved and mixed.

The spray pyrolysis setup had a pneumatic spray nozzle that was connected to a source of compressed air. This turned the precursor solution into small droplets. The glass substrates were put on a heated substrate holder that kept the temperature at 300°C. The precursor solution was sprayed at a steady flow rate during deposition, and the distance between the nozzle and

the substrate was set to make sure that the droplets were evenly spread out. When the aerosol droplets hit the heated substrate surface, they broke down thermally, which caused pyrolytic reactions that made CdS thin films. After deposition, the films were left to cool down to room temperature on their own. The films that came out of this process stuck well to the substrates, covered them evenly, and had smooth surfaces. The thickness of the films was changed by changing the spray time and the amount of precursor. Fig. 1 shows schematic representation of the spray pyrolysis deposition setup used for thin films deposition.

2.2 Characterization Techniques

We used Siemens D5005 X-ray diffractometer with CuKα radiation (λ=1.542 Å) in the 2θ range of 20°–80° to look at the structural properties of the deposited pure and Al-doped CdS thin films. The Debye–Scherrer equation is used to figure out the size of the crystallites and Bragg's law to determine the interplanar spacing. We compared the diffraction patterns with standard JCPDS data to make sure that the phase was formed and the crystallographic orientation was correct. Scanning electron microscopy (SEM) was used to look at the surface morphology and microstructural features of the thin films. Energy-dispersive X-ray spectroscopy (EDS) connected to the SEM system confirmed the elemental makeup and successful addition of Al dopant to the CdS lattice.

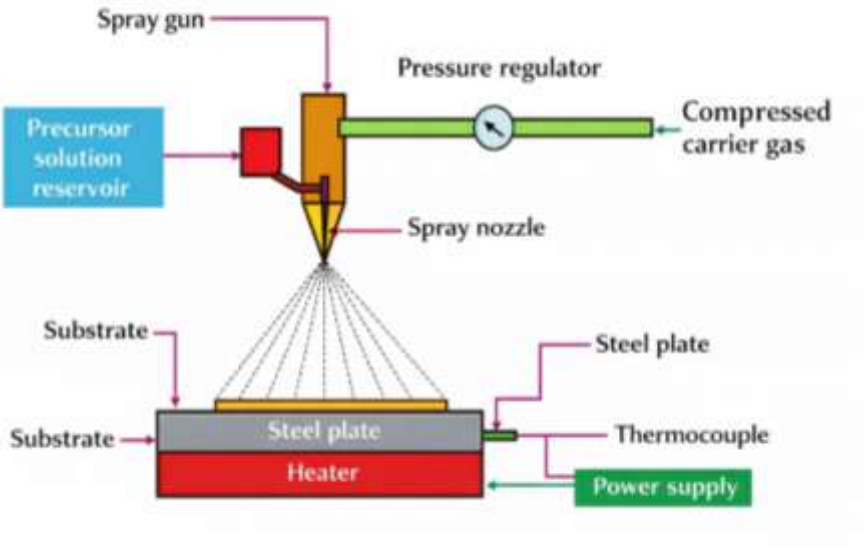

Fig. 1: Schematic representation of the spray pyrolysis setup.

3. Result and discussion

3.1. Formation of CdS Thin Films

During spray pyrolysis, atomised precursor droplets quickly evaporate the solvent and break down thermally when they hit the heated substrate. This makes pure and Al-doped CdS thin films. Cadmium acetate breaks down when it gets hot, making cadmium oxide, and thiourea breaks down, releasing sulphur species. The reactions that happen are shown as []:

$$Cd(CH_3COO)_2 \cdot 2H_2O \xrightarrow{\Delta} CdO + 2CH_3COOH + H_2O$$

$$CS(NH_2)_2 \xrightarrow{\Delta} H_2S + \text{volatile products}$$

$$CdO + H_2S \xrightarrow{\Delta} CdS + H_2O$$

These reactions result in the nucleation and growth of CdS crystallites on the substrate surface. The deposited CdS thin films are uniform, light yellow in colour, highly adhesive, smooth and reflecting.

3.2. Thickness Measurement:

The amount of material deposited can be controlled by several factors such as deposition time, the deposition rates or amount of material used in the process. The thickness of the as-prepared CdS films with Al doped were estimated using the weight difference method. The relationship used to calculate thickness (t) was [10]:

$$t = \frac{\Delta m}{A \times \rho} \qquad (1)$$

Where 'Δm' is weight difference between before and after the deposition of substrate, 'A' area of the deposited substrate and ρ is the density of deposited material (CdS = 4.826 g/cm^3) material. The values of thickness of deposited films were listed in Table 1. The thickness of the films was 2.125 μm and 1.842 μm for pure and 1% Al-doped CdS thin films.

3.3. Structural analysis

The X-ray diffraction (XRD) patterns of pure CdS and 1% Al-doped CdS thin films are shown in Fig. 2(a) and 2(b), respectively. The diffraction peaks seen in the pure CdS sample can be linked to the (220) and (400) crystallographic planes, which shows that polycrystalline CdS with good crystallinity has formed [11]. When Al is added (1%), the CdS peaks that are characteristic of the (220) and (400) planes stay the same. This shows that the host CdS crystal structure stays the same after doping. Also, a weak peak that corresponds to the (311) plane of Al can be seen in the doped sample, which shows that Al was successfully added to the CdS matrix [12]. After doping, there is a small change in the intensity of the peak and the

background scattering. This could be because Al incorporation causes lattice distortion, defect formation, and a decrease in crystallite size. The lack of additional impurity peaks indicates the absence of secondary phases, thereby confirming the structural stability of CdS upon Al doping [13].

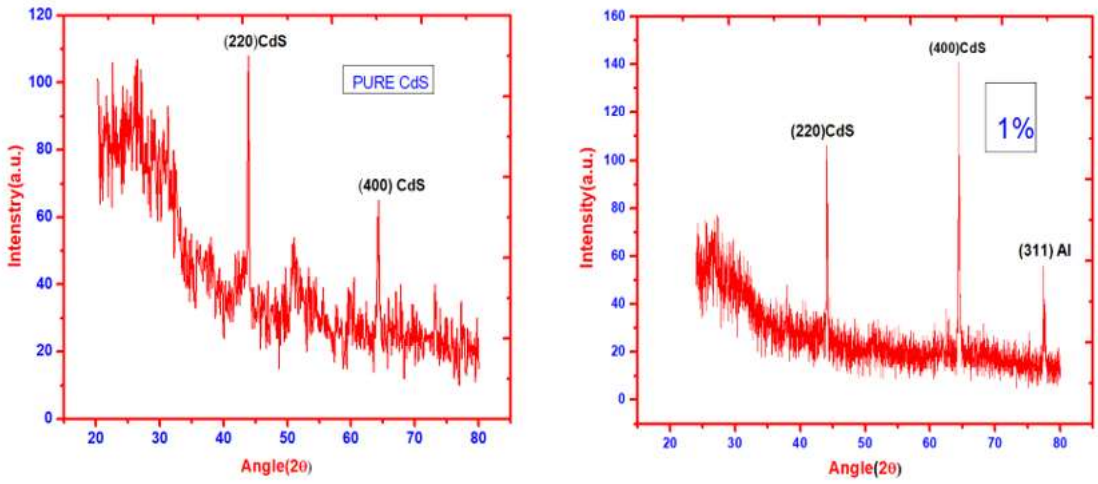

Fig. 2: XRD of pure CdS (left) and 1% Al-doped CdS (right) thin films.

From the position of different peaks and by the Bragg condition [14]:

$$n\lambda = 2dsin\theta \quad (2)$$

where n is the order of diffraction, λ the wavelength of the incident X-rays, d the distance between the plans parallel to the axis of the incident beam.

The average size of the crystallites (D) has been calculated using Scherer's equation as [15]:

$$D = \frac{K\lambda}{\beta cos\theta} \quad (3)$$

where the constant K is a shape factor usually = 0.94, λ is of X-ray wavelength (λ =1.542 Å), β is the full-width at half maximum (FWHM) of the peak which has maximum intensity and θ is the Bragg's angle.

Table 1 shows the structural parameters that were found from the X-ray diffraction analysis of pure and 1% Al-doped CdS thin films. These include the observed diffraction planes, the calculated and standard 2θ values, the interplanar spacing (d), and the average crystallite size (D). Two strong diffraction peaks for the pure CdS thin film can be seen at calculated 2θ values of 43.1092° and 64.285°, which correspond to the (220) and (400) planes [16], [17]. These numbers are close to the standard JCPDS values (43.99° and 64.08°), which shows that crystalline CdS has formed without any other phases. The interplanar spacings were found to be 2.0639 Å and 1.4452 Å, respectively. Using the Debye–Scherrer equation [18], we found

that the average crystallite size for pure CdS was 72 nm Å. This means that the crystallite domains are relatively large and the crystals are of good quality [19].

When CdS thin films are doped with 1% Al, the characteristic CdS peaks for the (220) and (400) planes are still there. This means that Al doping does not change the structure of the host CdS crystal. There is, however, a noticeable change in the calculated 2θ value of the (220) plane, which is now at a higher angle (44.62°) than the standard value (43.99°). This suggests that the lattice is contracting because smaller Al^{3+} ions are replacing Cd^{2+} ions. Also, there is a weak diffraction peak that corresponds to the (311) plane at a calculated 2θ value of 77.89°. This value is very close to the standard value of 77.36°, which shows that Al has been successfully added to the CdS lattice. The interplanar spacings for the doped sample are a little smaller than those for the pure CdS film. This is more evidence that there are lattice distortion and strain. The average size of the crystallites in the 1% Al-doped CdS film is now 552.6 Å. This shows that adding Al stops crystallites from growing and creates more defect sites.

In general, the structural parameters obtained from XRD analysis show that Al doping causes the size of the crystallites to decrease, the lattice to distort, and the peaks to shift without creating secondary phases. These changes to the structure are likely to have a big effect on the optical and electrical properties of CdS thin films. This makes Al-doped CdS a good choice for optoelectronic uses.

Table 1: Structural parameters of pure and Al doped CdS thin films.

Sample	Planes (hkl)	2θ (calculated) (º)	2θ (Standard) (º)	d (Å)	D (nm)
Pure CdS	220	43.10	43.99	2.0639	72.6
	400	64.28	64.08	1.4452	
1% Al-CdS	220	44.62	43.99	2.0127	55.2
	400	64.2851	64.086	1.4452	
	311	77.8991	77.360	1.2480	

3.4. Morphological Analysis

Fig. 3 shows the scanning electron microscope (SEM) image of the Al-doped CdS thin film. Fig. 3 displays a densely packed surface morphology characterised by irregularly shaped granules with prominent agglomeration. The particle size distribution, as depicted in the image, primarily ranges from approximately 395 to 675 nm, thereby confirming the nanostructured

nature of the film. The existence of interconnected granules and clusters indicates greater surface roughness and an expanded surface area, which can be ascribed to the incorporation of Al dopant affecting the nucleation and growth mechanisms. Such a dense yet detailed morphology is advantageous for optoelectronic and sensing applications, as it can enhance charge transport and surface-related interactions.

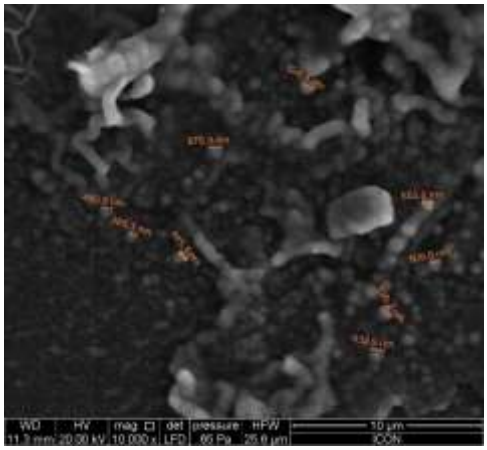

Fig. 3: SEM image of 1% Al-doped CdS thin film.

3.5. Elemental analysis

Fig. 4 illustrate the Energy Dispersive X-ray Spectroscopy (EDS) spectrum of Al-doped CdS thin film. EDS spectra of the film verify the elemental composition of the Al-doped CdS sample. Prominent peaks associated with cadmium (Cd) and sulphur (S) confirm the formation of CdS, while the detection of a distinct aluminium (Al) peak verifies the successful integration of Al dopant into the CdS matrix. The evaluated elemental atomic percentage are 49.18 at. % for Cd, 49.8 at. % for S and 1.02 at. % respectively.

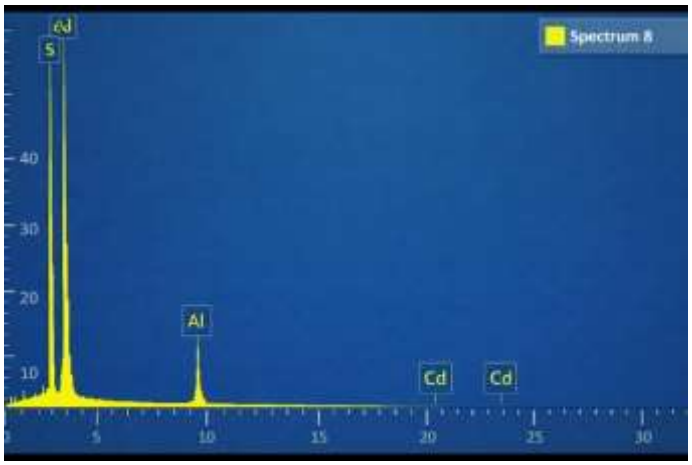

Fig. 4: EDS spectra of 1% Al-doped CdS thin film.

3.6 Optical analysis:

The optical energy band gap of the deposited CdS thin films was determined using Tauc's relation, given by Eq. (4), where α is the absorption coefficient, hν represents the photon energy, A is a proportionality constant, and n equals ½ for direct allowed electronic transitions [22].

$$(\alpha h\upsilon)^n = (h\upsilon - E_g) \quad (4)$$

As shown in Fig. 3(b), the band gap energy (E_g) was obtained by extrapolating the linear region of the $(\alpha h\nu)^2$ versus hν plot to the energy axis for films deposited at different substrate temperatures. The estimated optical band gap values increases from 2.40 eV to 2.50 eV with dopant [21]. This increase in band gap is consistent with reported literature, where the band gap is inversely related to grain size. The observed variation in E_g may be attributed to grain growth, the formation of localized sub-energy levels near the conduction band, and increased lattice disorder in the CdS thin films [20] [24].

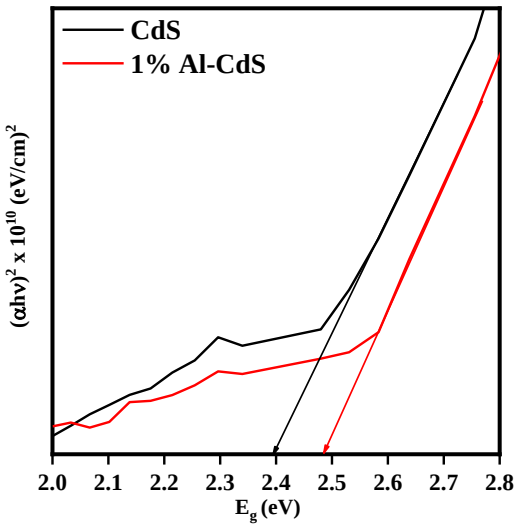

Fig 5: Tauc's plot for CdS and 1% Al-doped CdS.

4. Conclusion

Al doped CdS nanocrystalline thin films were successfully deposited on glass substrates using a simple and cost-effective spray pyrolysis technique with Al concentrations 0 and 1 at. %. Structural analysis by XRD confirmed the formation of polycrystalline CdS with a preferred (111) orientation for all doping levels, indicating that Al incorporation does not alter the

fundamental crystal structure of CdS. The crystallite size was found to be in the nanometre range, with a value of 72 nm and 55 nm for films 0 and 1 at. % Al. SEM observations revealed that the films possess a uniform and compact surface morphology composed of densely packed nanograins, demonstrating good surface coverage and film continuity. EDS analysis verified the successful incorporation of aluminum into the CdS lattice, and the elemental composition closely matched the intended dopant concentrations. Overall, the results indicate that spray pyrolysis is an effective and scalable deposition method for producing high-quality Al-doped CdS thin films with controlled structural and compositional characteristics.

References

[1] S. S. Kawar and B. H. Pawar, “Synthesis and characterization of CdS n-Type of semiconductor thin films having nanometer grain size,” *Chalcogenide Lett.*, vol. 6, no. 5, pp. 219–225, 2009.

[2] M. Shkir, “Enhanced luminescence and visible-light photodetection performance of novel Bi, Sm, and Bi:Sm co-doped CdS nanostructured thin films developed via nebulizer spray pyrolysis technique,” *J. Sol-Gel Sci. Technol. 2024 1132*, vol. 113, no. 2, pp. 331–343, Nov. 2024, doi: 10.1007/S10971-024-06622-3.

[3] W. Ismail, G. Ibrahim, M. A. Habib, O. K. Alduaij, M. Abdelfatah, and A. El-Shaer, “Advancement of Physical and Photoelectrochemical Properties of Nanostructured CdS Thin Films toward Optoelectronic Applications,” *Nanomater. 2023, Vol. 13, Page 1764*, vol. 13, no. 11, p. 1764, May 2023, doi: 10.3390/NANO13111764.

[4] A. El-Shaer, S. Ezzat, M. A. Habib, O. K. Alduaij, T. M. Meaz, and S. A. El-Attar, “Influence of Deposition Time on Structural, Morphological, and Optical Properties of CdS Thin Films Grown by Low-Cost Chemical Bath Deposition,” *Crystals*, vol. 13, no. 5, p. 788, May 2023, doi: 10.3390/CRYST13050788/S1.

[5] M. Kamalian, E. Hasani, L. Babazadeh Habashi, and M. Gholizadeh Arashti, “Impact of post-deposition annealing on the optical, electrical, and structural properties of CdS thin films for solar cell applications,” *Phys. B Condens. Matter*, vol. 674, p. 415524, Feb. 2024, doi: 10.1016/J.PHYSB.2023.415524.

[6] K. Haunsbhavi *et al.*, “Effect of doping (Sn and In) on CdS thin films for ammonia sensing at room temperature,” *Sensors Actuators A Phys.*, vol. 376, p. 115567, Oct. 2024, doi: 10.1016/J.SNA.2024.115567.

[7] E. Gavrishchuk *et al.*, “Spray pyrolysis deposited Cr and In doped CdS films for laser application,” *Opt. Mater. (Amst).*, vol. 117, p. 111153, Jul. 2021, doi: 10.1016/J.OPTMAT.2021.111153.

[8] J. Hakami, “Highly induced photosensing behavior of Erbium (Er), Yttrium (Y) and Terbium (Tb) doped nanostructured Cadmium Sulphide (CdS) thin films prepared by nebulizer spray pyrolysis method,” *J. Alloys Compd.*, vol. 924, p. 166577, Nov. 2022, doi: 10.1016/J.JALLCOM.2022.166577.

[9] K. Hari Prasad, S. Vinoth, V. Ganesh, and R. Ade, “Fabrication of Al and La co-doped

CdS thin film for ammonia gas-sensing application through low-cost nebulizer spray pyrolysis technique," *Appl. Phys. A 2024 1303*, vol. 130, no. 3, pp. 204-, Feb. 2024, doi: 10.1007/S00339-024-07355-4.

[10] A. D. Kanwate, L. H. Kathwate, V. R. Panse, A. Saregar, and S. R. Choubey, "Effect of thickness on structural, morphological and optical properties of spray deposited CdSe0.3Te0.7 thin films," *J. Mater. Sci. Mater. Electron. 2023 3435*, vol. 34, no. 35, pp. 2254-, Dec. 2023, doi: 10.1007/S10854-023-11578-1.

[11] M. G. Faraj, H. H. Karim, A. F. Qader, I. N. Qader, and R. T. Ali, "Effect of molarity on the optical and structural properties of CdS thin films deposited by spray pyrolysis on flexible plastic substrates," *J. Mater. Sci. Mater. Electron. 2024 3532*, vol. 35, no. 32, pp. 2069-, Nov. 2024, doi: 10.1007/S10854-024-13839-Z.

[12] S. Sathish Kumar, S. Valanarasu, A. Vimala Juliet, R. S. Rimal Isaac, and V. Ganesh, "Effect of coating temperature on the properties of CdS thin films coated by nebulizer spray pyrolysis method for photodetection applications," *J. Photochem. Photobiol. A Chem.*, vol. 458, p. 115949, Jan. 2025, doi: 10.1016/J.JPHOTOCHEM.2024.115949.

[13] M. Vishwas, K. S. Shamala, and S. B. Gandla, "Comparison of optical properties of CdS thin films synthesized by spray pyrolysis and thermal evaporation method," *J. Opt. 2022 513*, vol. 51, no. 3, pp. 736–740, May 2022, doi: 10.1007/S12596-022-00887-Z.

[14] G. Kartopu, Q. Fan, O. Oklobia, and S. J. C. Irvine, "Combinatorial study of the structural, optical, and electrical properties of low temperature deposited Cd1-xZnxTe ($0 \leq x \leq 1$) thin films by MOCVD," *Appl. Surf. Sci.*, vol. 540, no. P2, p. 148452, 2021, doi: 10.1016/j.apsusc.2020.148452.

[15] V. S. Chandak, L. H. Kathwate, M. B. Kumbhar, and P. M. Kulal, "Spray deposited high performance Fe-doped ZnO ethanol sensor operating at low temperatures," *J. Ind. Eng. Chem.*, no. January, pp. 1–15, 2025, doi: 10.1016/j.jiec.2025.01.053.

[16] A. S. Najm *et al.*, "An in-depth analysis of nucleation and growth mechanism of CdS thin film synthesized by chemical bath deposition (CBD) technique," *Sci. Reports 2022 121*, vol. 12, no. 1, pp. 15295-, Sep. 2022, doi: 10.1038/s41598-022-19340-z.

[17] A. S. Najm *et al.*, "Mechanism of Chemical Bath Deposition of CdS Thin Films: Influence of Sulphur Precursor Concentration on Microstructural and Optoelectronic Characterizations," *Coatings 2022, Vol. 12, Page 1400*, vol. 12, no. 10, p. 1400, Sep. 2022, doi: 10.3390/COATINGS12101400.

[18] L. H. Kathwate, V. S. Chandak, Y. S. Mane, S. D. Lokhande, M. B. Awale, and A. D. Kanwate, "High-performance formaldehyde sensor based on Al-doped ZnO nanorods prepared by chemical bath deposition," *Ceram. Int.*, Apr. 2025, doi: 10.1016/J.CERAMINT.2025.04.120.

[19] M. Shkir and T. Alshahrani, "Engineering the physical properties of CdS thin films through incorporation of Fe dopant for photodetector applications," *J. Phys. Chem. Solids*, vol. 177, p. 111282, Jun. 2023, doi: 10.1016/J.JPCS.2023.111282.

[20] H. K. Abbood and N. A. Ali, "Studying the effect of cadmium chloride and thiourea concentrations on the structural and optical properties of CdS films deposited using the spray pyrolysis technique," *J. Opt. 2023 534*, vol. 53, no. 4, pp. 3441–3452, Oct. 2023, doi: 10.1007/S12596-023-01444-Y.

[21] S. Yılmaz, M. Tomakin, I. Polat, and E. Bacaksız, “Facile synthesis and characterization of CdS thin films doped by yttrium atoms,” *Appl. Phys. A 2023 1298*, vol. 129, no. 8, pp. 579-, Jul. 2023, doi: 10.1007/S00339-023-06869-7.

[22] H. A. Farroh, R. A. Zaghlool, and M. Boshta, “Gamma radiation effect on the structural and optical properties of CdS thin films prepared by spray pyrolysis technique,” *Phys. Scr.*, vol. 99, no. 1, p. 015943, Dec. 2023, doi: 10.1088/1402-4896/AD1637.

[23] D. I. Halge *et al.*, “Development of highly sensitive and ultra-fast visible-light photodetector using nano-CdS thin film,” *Appl. Phys. A 2021 1276*, vol. 127, no. 6, pp. 446-, May 2021, doi: 10.1007/S00339-021-04611-9.

[24] A. Kathalingam, S. Valanarasu, T. Ahamad, S. M. Alshehri, and H. S. Kim, “Spray pressure variation effect on the properties of CdS thin films for photodetector applications,” *Ceram. Int.*, vol. 47, no. 6, pp. 7608–7616, Mar. 2021, doi: 10.1016/J.CERAMINT.2020.11.100.